Agricultural and Forest Meteorology 214–215 (2015) 293–305

Contents lists available at ScienceDirect

Agricultural and Forest Meteorology

journal homepage: www.elsevier.com/locate/agrformet

Biophysical controls on carbon and water vapor fluxes across a grassland climatic gradient in the United States

Pradeep Wagle[a,*], Xiangming Xiao[a,b], Russell L. Scott[c], Thomas E. Kolb[d], David R. Cook[e], Nathaniel Brunsell[f], Dennis D. Baldocchi[g], Jeffrey Basara[h], Roser Matamala[i], Yuting Zhou[a], Rajen Bajgain[a]

[a] Department of Microbiology and Plant Biology, Center for Spatial Analysis, University of Oklahoma, Norman, OK 73019, USA
[b] Institute of Biodiversity Science, Fudan University, Shanghai 200433, China
[c] USDA-ARS, Southwest Watershed Research Center, Tucson, AZ 85719, USA
[d] School of Forestry, Northern Arizona University, Flagstaff, AZ 86011, USA
[e] Environmental Research Division, Argonne National Laboratory, Argonne, IL 60439, USA
[f] Department of Geography – Atmospheric Sciences Program, University of Kansas, Lawrence, KS 66045, USA
[g] Department of Environmental Science, Policy, & Management, University of California Berkeley, Berkeley, CA 94720, USA
[h] School of Meteorology and Oklahoma Climatological Survey, University of Oklahoma, Norman, OK 73019, USA
[i] Biosciences Division, Argonne National Laboratory, Argonne, IL 60439, USA

ARTICLE INFO

Article history:
Received 5 March 2015
Received in revised form 15 June 2015
Accepted 25 August 2015

Keywords:
Ecosystem water use efficiency
Eddy covariance
Enhanced vegetation index
Evapotranspiration
Grasslands
Gross primary production

ABSTRACT

Understanding of the underlying causes of spatial variation in exchange of carbon and water vapor fluxes between grasslands and the atmosphere is crucial for accurate estimates of regional and global carbon and water budgets, and for predicting the impact of climate change on biosphere–atmosphere feedbacks of grasslands. We used ground-based eddy flux and meteorological data, and the Moderate Resolution Imaging Spectroradiometer (MODIS) enhanced vegetation index (EVI) from 12 grasslands across the United States to examine the spatial variability in carbon and water vapor fluxes and to evaluate the biophysical controls on the spatial patterns of fluxes. Precipitation was strongly associated with spatial and temporal variability in carbon and water vapor fluxes and vegetation productivity. Grasslands with annual average precipitation <600 mm generally had neutral annual carbon balance or emitted small amount of carbon to the atmosphere. Despite strong coupling between gross primary production (GPP) and evapotranspiration (ET) across study sites, GPP showed larger spatial variation than ET, and EVI had a greater effect on GPP than on ET. Consequently, large spatial variation in ecosystem water use efficiency (EWUE = annual GPP/ET; varying from 0.67 ± 0.55 to 2.52 ± 0.52 g C mm^{-1} ET) was observed. Greater reduction in GPP than ET at high air temperature and vapor pressure deficit caused a reduction in EWUE in dry years, indicating a response which is opposite than what has been reported for forests. Our results show that spatial and temporal variations in ecosystem carbon uptake, ET, and water use efficiency of grasslands were strongly associated with canopy greenness and coverage, as indicated by EVI.

© 2015 Elsevier B.V. All rights reserved.

1. Introduction

In the past two decades, eddy covariance systems have been established in several grassland sites in the United States (U.S.) for investigations of processes controlling carbon and water vapor fluxes, and site specific results have been reported (Baldocchi et al., 2004; Fischer et al., 2012; Krishnan et al., 2012; Ma et al., 2007; Scott et al., 2010; Suyker et al., 2003). However, these observation networks cover only a small portion of grasslands. Sole reliance on individual sites may lead to biased estimates of fluxes at large scales (Biondini et al., 1991; Rahman et al., 2001). The broad distribution of grasslands across contrasting climate and management gradients adds to the complexity of measuring and modeling of fluxes, and understanding the vulnerability of ecosystems to environmental change. It is commonly accepted that ecosystem responses to changes in climatic-forcing variables such as precipitation, temperature, and CO_2 concentration are nonlinear (Burkett et al., 2005; Gill et al., 2002). Grasslands are considered ideal for rainfall manipulation studies because they are highly responsive to interannual variability in precipitation (Knapp et al., 2002). However,

* Corresponding author.
E-mail address: pradeep.wagle@ou.edu (P. Wagle).

http://dx.doi.org/10.1016/j.agrformet.2015.08.265
0168-1923/© 2015 Elsevier B.V. All rights reserved.

precipitation manipulation experiments at individual sites rarely capture this nonlinearity as they tend to have few (only two or three) treatments different from the control and do not manipulate temperature, which can co-vary with precipitation. Flux tower sites now allow comparative analysis, synthesis, modeling, and upscaling of site-level flux measurements (Falge et al., 2002; Gilmanov et al., 2003, 2010; Turner et al., 2003; Xiao et al., 2014). Synthesis of flux data from multiple sites across a climatic gradient allows analysis of the influences of a wider range environmental condition compared with manipulative studies at a single site. Several studies have investigated spatial variability of carbon fluxes (Churkina et al., 2005; Gilmanov et al., 2005; Kato and Tang, 2008; Law et al., 2002; Soussana et al., 2007; Yu et al., 2013; Yuan et al., 2009). These studies have shown that spatial variability of carbon fluxes is significantly correlated with mean annual temperature (MAT) and precipitation (MAP). However, most of the synthesis studies assembled all biomes together, which masked differences in response over spatial gradients within a biome type, such as grasslands. Compared to carbon fluxes, spatial variability in water vapor fluxes and water use efficiency at the ecosystem level, and the mechanistic understanding of the underlying controlling mechanisms in grasslands is still unclear. In addition, very little is known regarding the relative sensitivity of different grassland communities (C_4, mixed C_3/C_4, and C_3 dominant) across broadly distributed grasslands to climate. High frequency eddy covariance measurements allow calculation of net ecosystem CO_2 exchange (NEE), evapotranspiration (ET), gross primary production (GPP), ecosystem respiration (ER), and synthetic metrics such as ecosystem water use efficiency (EWUE, which reflects the tradeoff between water loss and carbon uptake in carbon assimilation process), thereby facilitating investigation of responses of carbon and water vapor fluxes to environmental drivers (Huxman et al., 2004; Law et al., 2002).

Satellite remote sensing provides a feasible approach for monitoring vegetation dynamics at ecosystem to global scales (Myneni et al., 1997; Zhang et al., 2003). A better understanding of phenological patterns of vegetation and their drivers is essential to improve climate and biogeochemical cycle models and also to better simulate the exchange of carbon and water vapor fluxes between land surface and the atmosphere (Running and Hunt, 1993). Previously, phenological dynamics have been shown to play a vital role in the variability of carbon and water vapor fluxes at the ecosystem scale for a broad range of ecosystems (DeForest et al., 2006; Hutyra et al., 2007; Ma et al., 2013; Richardson et al., 2010; Wagle et al., 2015). However, the major drivers of spatial variability of phenological metrics and the role of phenological dynamics on spatial variability of fluxes have not been specifically examined for broadly distributed grasslands in the U.S. This greatly hampers our understanding of the impacts of future climate change on phenological dynamics and the carbon and water budgets of U.S. grasslands. Further, an establishment of a robust relationship between tower fluxes and remotely sensed data can facilitate extrapolation of site-level fluxes to obtain regional estimates of carbon and water budgets across complex landscapes (Gilmanov et al., 2005; Xiao et al., 2008).

This study covers 12 AmeriFlux grassland sites that represent the distribution of grasslands within the conterminous U.S., including C_4 dominated semi-arid shortgrass prairie of the Southwest (AZ), C_3 dominated Mediterranean grassland (CA), C_3/C_4 mixed temperate grassland of the Northwest (MT) and Southeast (MS), C_4 dominated temperate continental tallgrass prairie of the Midwest (IL, KS) and South Central (OK), and C_3/C_4 mixed humid continental grassland of the Midwest (SD). The objectives of this study were: (1) to analyze the spatial variability in grassland carbon and water vapor fluxes, (2) examine whether a satellite measurement of green biomass (as quantified by the Moderate Resolution Imaging Spectroradiometer (MODIS) enhanced vegetation index, EVI) captures the observed spatial variability in carbon and water vapor fluxes, and (3) determine the responses of GPP and ET to major climatic variables. The time series measurements quantify the conditional statistics associated with seasonal changes in climatic variables and the results provide important insights about predicting the impact of climate change on biosphere–atmosphere feedbacks of grasslands under current and future climatic conditions.

2. Materials and methods

2.1. Site descriptions

The 12 grassland sites used in this study (Fig. S1) cover a broad range of geographic location, grassland type (warm-season C_4 dominant, mixed C_3 and C_4 species, and cool-season C_3 dominant), and climate (semi-arid, temperate/temperate continental, humid continental, and Mediterranean). Long term MAT ranged from 5 to 17 °C and MAP ranged from 345 to 1455 mm across sites. General site characteristics for the study sites are provided in Table 1. Detailed site information can be found in previous studies (see references in Table 1) or AmeriFlux website (http://ameriflux.ornl.gov/).

Supplementary Fig. S1 related to this article can be found, in the online version, at http://dx.doi.org/10.1016/j.agrformet.2015.08.265.

2.2. Meteorological, eddy flux, and MODIS EVI data

Site-specific climate data [i.e., air temperature (T_a), precipitation, volumetric soil water content (SWC), vapor pressure deficit (VPD)] and Level-4 eddy flux (half hourly, daily, and weekly) were acquired from the AmeriFlux website (http://ameriflux.ornl.gov/) or from published data by the site PI (R. Scott, Kendall grassland). Carbon and water vapor fluxes were measured at each site using the eddy covariance technique. GPP was derived by partitioning NEE data (Reichstein et al., 2005). Some study sites (Flagstaff Wildfire, El Reno burn and control, Fermi Prairie, Walnut, and Brookings) had a total of only 2–3 years of data and measurements were not available for the entire year (mainly missing during winter, non-growing season). In this case, NEE, GPP, ER, and ET data over the available period were averaged for the same date into a single composite year and integrated for the entire year to derive annual sums of NEE (NEE_{yr}), GPP (GPP_{yr}), ER (ER_{yr}), and ET (ET_{yr}) at each site. Moreover, due to data availability during most of the growing season, growing season sums of NEE (NEE_{GSL}), GPP (GPP_{GSL}), ER (ER_{GSL}), and ET (ET_{GSL}) at each site were also computed for each year. For the rest of the sites where multiple years of data were available for the entire year, annual and growing season sums of carbon fluxes and ET at each site were computed for each year. Since flux data were available for the peak growing season across all site-years, maximum values of fluxes (NEE_{max}, GPP_{max}, and ET_{max}) at each site were computed for each year.

The 8-day composite MODIS land surface reflectance (MOD09A1) data for single pixels (500 m × 500 m) containing the geo-location coordinates of a flux tower were downloaded from the data portal of the Earth Observation and Modeling Facility, the University of Oklahoma (http://eomf.ou.edu/visualization/). Although the spatial resolution of the MODIS pixels and flux tower footprints may vary, Fig. S2 shows that the MODIS pixels mostly cover uniform grasslands. Blue, green, red, and near infrared (nir) bands were used to derive EVI (Huete et al., 2002) as shown below:

$$\mathrm{EVI} = 2.5 \times \frac{\rho_{\mathrm{nir}} - \rho_{\mathrm{red}}}{\rho_{\mathrm{nir}} + (6 \times \rho_{\mathrm{red}} - 7.5 \times \rho_{\mathrm{blue}}) + 1} \quad (1)$$

where ρ is surface reflectance in the wavelength band. EVI, widely used as a proxy of canopy greenness, is an optimized version of normalized difference vegetation index (NDVI) to account for

Table 1
Description of vegetation types and climate at flux sites.

Climate	Site (State)	Latitude Longitude	Elevation (m) MAT (°C) MAP (mm)	Study period	Vegetation	Soil type	References
Semi-arid	Audubon (AZ)	31.5907 −110.5092	1469 14.7 475	2002–2006	Short-grass prairie (C_4) and perennial herbs	Sandy clay loam	Krishnan et al. (2012)
Semi-arid	Flagstaff Wildfire (AZ)	35.4454 −111.7718	2270 9 610	2005–2007	Short-grasses (C_3/C_4 mixed) with a few shrubs	Silt clay loam	Dore et al. (2008)
Semi-arid	Kendall (AZ)	31.7365 −109.9419	1531 17 345	2005–2009	Short-grass prairie (C_4) and C_3 shrubs	Sandy loam	Scott et al. (2010)
Temperate continental	El Reno Burn (OK)	35.5497 −98.0402	421 14.9 860	2005–2006	C_4 dominated tallgrass prairie	Norge silt loam	Fischer et al. (2012)
Temperate continental	El Reno Control (OK)	35.5465 −98.0401	421 14.9 860	2005–2006	C_4 dominated tallgrass prairie	Norge silt loam	Fischer et al. (2012)
Temperate continental	Fermi Prairie (IL)	41.8406 −88.2410	226 9.4 937	2005–2007	C_4 dominated tallgrass prairie	Silt clay loam	Matamala et al. (2008)
Temperate continental	Konza (KS)	39.0824 −96.5603	443 13 835	2007–2012	C_4 dominated tallgrass prairie	Silt clay loam	Brunsell et al. (2008)
Temperate continental	Walnut (KS)	37.5208 −96.8550	408 13.1 1054	2001–2004	Tallgrass prairie (C_3/C_4 mixed)	Silt clay loam	Song et al. (2005)
Humid continental	Brookings (SD)	44.3453 −96.8362	510 5.8 550	2004–2006	Mixed C_3 and C_4 species	Clay loam	Gilmanov et al. (2010)
Temperate	Fort Peck (MT)	48.3077 −105.1019	634 5.13 500	2000–2006 (missing 2002)	Mixed C_3 and C_4 species	Sandy loam	Gilmanov et al. (2010)
Temperate	Goodwin (MS)	34.2547 −89.8735	70 15.7 1455	2002–2006	Short-grasses (C_3/C_4) with scattered trees and shrubs	Silt loam	Gilmanov et al. (2010)
Mediterranean	Vaira (CA)	38.4067 −120.9507	129 15.9 498	2001–2007	Cool-season C_3 species and sparsely distributed oak trees	Very rocky silt loam	Baldocchi et al. (2004)

MAT, mean annual temperature; MAP, mean annual precipitation.

atmospheric noise variations and variable soil and canopy background influences (Huete et al., 2002).

Supplementary Fig. S2 related to this article can be found, in the online version, at http://dx.doi.org/10.1016/j.agrformet.2015.08.265.

To match the temporal resolution of EVI, we calculated 8-day composite values of fluxes and meteorological variables. We averaged 8-day composite values of NEE, GPP, ET, T_a, and SWC over the study period for the same date into a single composite year for each site to determine their mean seasonal patterns. Maximum values of EVI (EVI_{max}) during the growing season were computed for each year. The 8-day composite EVI values for the growing season were summed to derive growing season sum of EVI (EVI_{sum}) for each year.

2.3. Growing season length based on GPP and EVI

Growing season length based on GPP (GSL_{GPP}) was determined as the number of days for which GPP was >1 g C m^{-2} day^{-1} (Wagle et al., 2014). Carbon uptake period (CUP) was determined as the number of days of negative NEE (carbon uptake by the ecosystem) during the growing season (Wagle et al., 2015). If there were periods with GPP less than 1 g C m^{-2} day^{-1} or positive NEE during the growing season, those periods were excluded from GSL_{GPP} or CUP (for example see Brookings site in Table 2). To relate GSL_{GPP} from flux tower measurements, the growing season length (GSL_{EVI}) was determined based on EVI. The GSL_{EVI} was defined as the number of days the EVI was greater than the given threshold values for each site. The threshold values of EVI were determined when EVI started to increase at the beginning of the growing season and decreased after senescence. The threshold EVI values were ~0.12 at semi-arid sites (Audubon, Flagstaff, and Kendall) and Fortpeck, while they were ~0.20 at all other sites. To reduce the uncertainties in times series of EVI and interannual variations in the growing season length at individual sites (the green-up time of grassland links to timing of rainfall and spring temperature), we averaged 8-day composite EVI and carbon fluxes over the study period into a single composite year to produce mean 8-day time series of EVI and carbon fluxes, then determined GSL_{EVI}, GSL_{GPP}, and CUP.

2.4. Calculation of ecosystem water use efficiency (EWUE)

The EWUE for the annual scale ($EWUE_{yr}$) was calculated from the ratio of GPP_{yr} to ET_{yr}, while EWUE for the growing season ($EWUE_{GSL}$) was determined from the ratio of integrated GPP (GPP_{GSL}) to ET (ET_{GSL}) over the growing season. To assess the intrinsic link between GPP and ET via stomatal conductance at the ecosystem level, inherent ecosystem water use efficiency (IEWUE) was derived from the ratio of GPP to ET multiplied by VPD on daily time scales (Beer et al., 2009) and compared for selected sites

Table 2
Seasonal dynamics of carbon fluxes (net ecosystem CO_2 exchange, NEE and gross primary production, GPP), maximum rates of NEE (NEE_{max}, g C m^{-2} day^{-1}), GPP (GPP_{max}, g C m^{-2} day^{-1}), and evapotranspiration (ET_{max}, mm day^{-1}), and maximum (EVI_{max}) and seasonally integrated values (EVI_{sum}) of enhanced vegetation index at the 12 grassland sites.

Site	GSL_{EVI} (DOY)	CUP (DOY)	GSL_{GPP} (DOY)	NEE_{max} (±SD)	GPP_{max} (±SD)	ET_{max} (±SD)	EVI_{max} (±SD)	EVI_{sum} (±SD)
Audubon	185–305	217–257	209–257	−3.59 ± 1.65	5.51 ± 2.57	4.04 ± 1.16	0.32 ± 0.04	3.16 ± 0.24
Flagstaff Wildfire	105–313	121–153	121–273	−0.91 ± 0.34	4.45 ± 0.39	3.39 ± 0.66	0.30 ± 0.04	4.72 ± 0.22
Kendall	193–297	209–257	209–257	−2.73 ± 1.18	4.45 ± 1.45	3.30 ± 0.46	0.27 ± 0.08	2.49 ± 0.27
El Reno burn	97–305	113–217	105–289	−6.85 ± 2.3	13.74 ± 4.82	5.54 ± 0.09	0.54 ± 0.08	10.26 ± 1.33
El Reno control	97–297	113–217	97–289	−5.19 ± 0.23	11.02 ± 2.01	5.69 ± 0.3	0.55 ± 0.09	9.9 ± 1.28
Fermi Prairie	97–313	113–265	105–289	−9.50 ± 1.49	14.49 ± 1.85	5.64 ± 0.34	0.65 ± 0.06	11.68 ± 0.48
Konza	97–321	129–233	97–321	−9.10 ± 1.29	15.86 ± 2.63	7.61 ± 0.92	0.59 ± 0.07	10.31 ± 0.38
Walnut	89–313	113–273	105–289	−4.50 ± 0.77	10.63 ± 0.63	5.24 ± 0.8	0.53 ± 0.05	10.0 ± 0.27
Brookings	81–329	97–185 and 265–305	97–305	−5.35 ± 1.34	10.59 ± 1.62	8.13 ± 1.7	0.66 ± 0.1	13.21 ± 0.05
Fort Peck	97–265	105–169	105–225	−2.12 ± 1.24	4.38 ± 2.14	5.24 ± 2.86	0.31 ± 0.03	4.59 ± 0.17
Goodwin	25–337	33–273	33–313	−6.17 ± 2.29	12.68 ± 1.12	6.41 ± 2.43	0.62 ± 0.04	16.28 ± 0.22
Vaira	305–161	17–137	345–145	−5.41 ± 0.79	10.38 ± 0.60	3.81 ± 0.40	0.43 ± 0.04	8.04 ± 0.51

Maximum values of NEE, GPP, ET, and EVI at each site were first determined for an individual year, then averaged for the entire study period.
GSL_{EVI} and GSL_{GPP} are growing season lengths based on EVI and GPP, respectively. CUP is carbon uptake period.
The 8-day composite EVI values were summed (EVI_{sum}) for the period of GSL_{EVI} for an individual year, then averaged for the study period.

in different climate zones during dry years. To further examine the relative response of NEE, GPP, and ET to two major climatic variables (T_a and VPD) across study sites, half-hourly daytime (global radiation >5 W m^{-2}) NEE, GPP, and ET during the period of GSL_{GPP} (Table 2) for the entire study period were aggregated in 10 classes of increasing T_a and VPD, and plotted against T_a and VPD.

2.5. Statistical analysis

We performed correlation and regression analyses between fluxes, EVI, and major climatic variables to assess the degree of association between dependent and independent variables. The relationships with the highest level of significance (i.e., best fit functions) were selected. The coefficient of variation (CV) was calculated for annual and seasonal integrals and maximum values of fluxes and EVI across study sites to characterize the magnitudes of spatial variations.

3. Results

3.1. Climatic conditions across study sites

Air temperature showed similar seasonal patterns across study sites, while volumetric SWC showed different seasonal patterns among study sites (Fig. 1). Annual average SWC was below 20% at semi-arid sites, 25–35% at temperate and temperate-continental sites, 44% at Brookings (humid continental), and 18% at Vaira (Mediterranean). Annual average relative water content [$\theta_R = (\theta - \theta_{min})/(\theta_{max} - \theta_{min})$, where θ_{min} and θ_{max} are minimum and maximum values of soil water content observed at each site] was low at semi-arid sites (0.34 at Audubon, 0.39 at Flagstaff, and 0.34 at Kendall), while it was 0.43 at Vaira and >0.46 at other sites (up to 0.65 at Brookings) (data not shown).

Several study sites experienced drought during the study period. For example, annual rainfall in 2004 was 26% lower than in 2005 at Audubon. At El Reno, annual rainfall was ~30% below the annual average (860 mm, 1971–2000) in both years of the study period. However, growing season rainfall and SWC at El Reno were higher in 2005 than 2006 (Fischer et al., 2012). Annual rainfall in 2012 was 60% lower than in 2010 at Konza. Annual rainfall in 2001 was 33% lower than in 2003 at Fort Peck. The Goodwin site received more than normal rainfall in 2004 but experienced drought in 2005. At Vaira, annual rainfall in the hydrological year (July to June) of 2003–2004 was 44% lower than the hydrological year of 2004–2005.

3.2. Seasonality and magnitudes of EVI and carbon and water vapor fluxes, and climatic controls

To characterize the seasonal variation of grassland phenology, the mean seasonal cycles of EVI, GPP, and ET were determined (Fig. 2). The EVI generally began to increase rapidly at approximately DOY 100 (April) for the majority of the sites, reached peak values in summer (peak growth), and decreased during the plant senescence stage and approached the pre-CUP value (e.g., prior to DOY 100) near DOY 300 (end of October). However, different seasonal lengths, as indicated by seasonal dynamics of EVI, were observed at Audubon and Kendall (semi-arid grasslands: DOY 180–300, corresponding to the summer rainy season), Vaira (Mediterranean grassland: ~DOY 300–160, with EVI_{max} occurring in spring), and Goodwin (temperate: ~DOY 25–335). Table 2 shows that mean EVI_{max} ranged from 0.27 ± 0.08 (Kendall) to 0.66 ± 0.1 (Brookings) and mean seasonal EVI_{sum} ranged from 2.49 ± 0.27 (Kendall) to 16.28 ± 0.22 (Goodwin), with CV of 31 and 48% across sites, respectively. The across-site analysis shows that EVI_{max} was strongly correlated with annual average θ_R ($R^2 = 0.70$, $P < 0.001$) but not with seasonal average θ_R ($R^2 = 0.12$, $P = 0.27$). Similarly, mean seasonal EVI_{sum} was strongly correlated with spatial variation in annual average θ_R ($R^2 = 0.67$, $P = 0.001$) than seasonal average θ_R ($R^2 = 0.17$, $P = 0.18$). Annual average θ_R and MAP together explained 90% ($P < 0.0001$) of spatial variation in mean seasonal EVI_{sum}.

The seasonal dynamics of carbon and water vapor fluxes also corresponded well with the vegetation dynamics because the fluxes began to increase after the grasses greened up, peaked at the maturity stage, and declined after senescence (Fig. 2). The GSL_{GPP} varied from only about 1.5 months (from end of July to mid-September) at semi-arid sites (Audubon and Kendall grasslands) to about nine months (from the starting of February to early November) at Goodwin (Table 2). Similarly, CUP was the longest (eight months) at Goodwin and the shortest at Audubon (41 days) as CUP was strongly correlated with GSL_{GPP} ($R^2 = 0.65$, $P < 0.001$) and MAP ($R^2 = 0.72$, $P < 0.001$). As expected, strong correlations were observed between GPP_{yr} or GPP_{GSL} and GSL_{GPP} (both: $R^2 = 0.79$, $P < 0.001$), and between CUP and NEE_{yr} ($R^2 = 0.66$, $P = 0.001$) or NEE_{GSL} ($R^2 = 0.56$, $P = 0.005$). Different magnitudes of NEE, GPP, and ET were observed across study sites (Table 2), with CV of 51%, 42%, and 29%, respectively, indicating a larger spatial variability of NEE and GPP than of ET. Annual average θ_R explained 22% ($P = 0.11$), 33% ($P = 0.05$), and 74% ($P < 0.0001$) of spatial patterns in NEE_{max}, GPP_{max}, and ET_{max}, respectively.

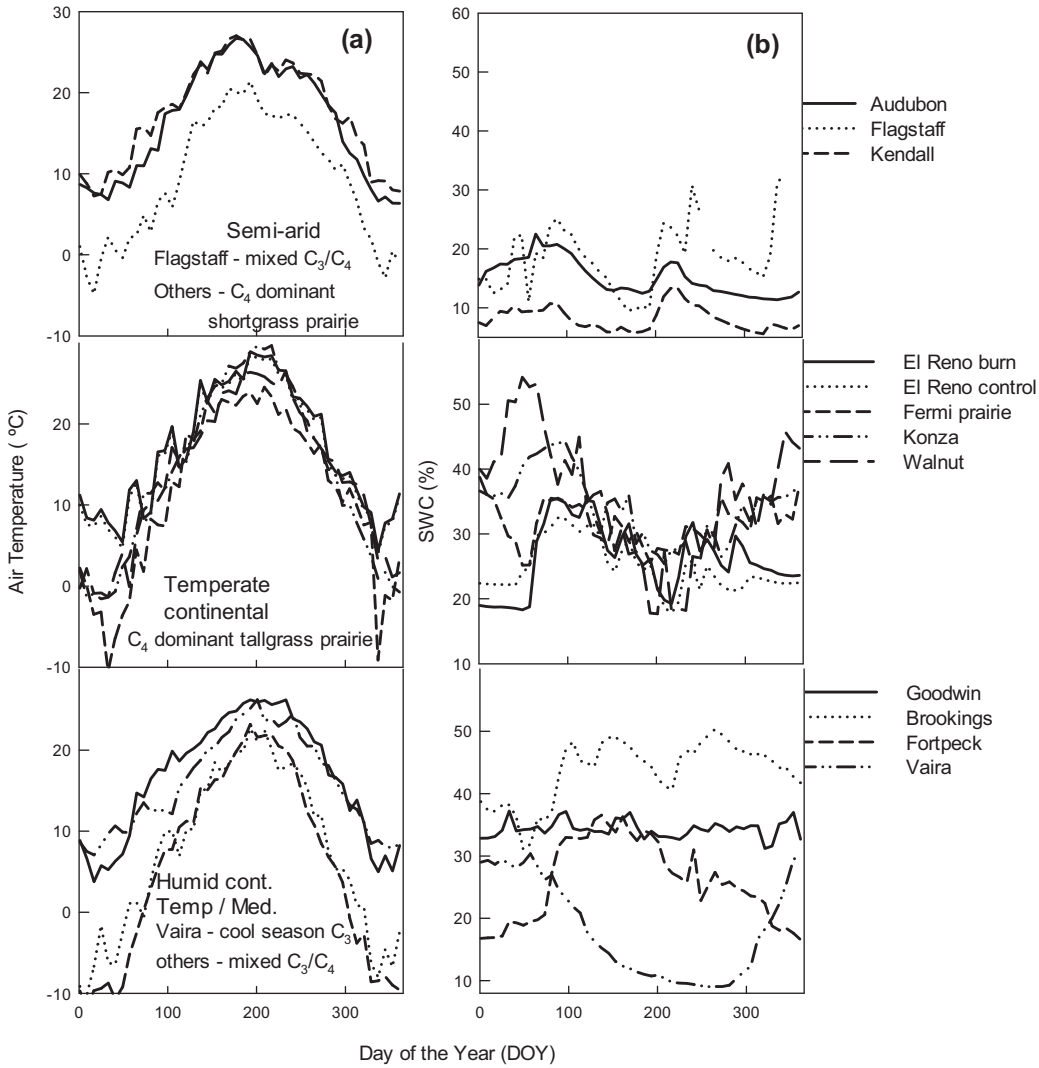

Fig. 1. Mean seasonal dynamics (8-day composite values) of annual air temperature and near surface volumetric soil water content (SWC) at the 12 grassland sites. Data over the study period were composited into a single year for each site to determine the mean seasonal patterns.

3.3. Variability in carbon and water budgets

Large variability in annual and seasonal sums of NEE, GPP, and ET was observed across study sites (Table 3), with CV of 164%, 54%, and 39%, respectively, on an annual scale and 93%, 58%, and 46%, respectively, on the seasonal scale. Average NEE_{yr} across study sites showed a net carbon uptake by grasslands, -76 ± 125 ($\pm$SD) g C m^{-2} year^{-1}, but with larger variability than the uptake itself. The spatial variation in NEE_{yr} was more strongly related to the variation in GPP_{yr} ($R^2 = 0.55$, $P = 0.006$) than to ecosystem respiration (ER_{yr}, $R^2 = 0.33$, $P = 0.05$). Annual and seasonal sums of carbon fluxes and ET tended to be lower in regions with smaller precipitation as fluxes showed positive and nonlinear relationship with precipitation (Fig. 3). Results show that GPP, ER, and ET were similar for the site-years with approximately >800 mm of annual precipitation and >600 mm of seasonal precipitation. The across-site analysis shows that annual average θ_R explained 53% ($P = 0.01$) of NEE_{GSL}, 55% ($P < 0.01$) of NEE_{yr}, 72% ($P < 0.001$) of GPP_{GSL} and ER_{GSL}, 75% ($P < 0.001$) of GPP_{yr}, and 67% ($P = 0.002$) of ER_{yr} when the Brookings site was excluded. Annual average θ_R explained 77% ($P < 0.001$) and 74% ($P < 0.001$) of spatial variations in ET_{GSL} and ET_{yr}, respectively.

In addition to spatial variability, grasslands showed large inter-annual variability in carbon uptake potential in response to climate forcing (i.e., drought) and disturbances (i.e., fire, invasion) or the biological legacy effects of extensive vegetation growth in the previous year. For example, there was a net carbon uptake of 167 g C m^{-2} year^{-1} at the Audubon site in 2005 when annual and seasonal rainfall was over 350 and 250 mm, respectively, while the site emitted more carbon than it assimilated for the rest of the years. The Konza site, which had a consistent carbon uptake from 2007 to 2011, emitted more carbon than it assimilated in the drought year of 2012. The Flagstaff Wildfire site emitted more carbon than it assimilated both on seasonal and annual time scales for the entire study period because of the wildfire a decade before the flux measurements that killed all trees. The Audubon site emitted more carbon in 2003 after the wildfire in 2002. The carbon uptake by the Fermi Prairie site declined dramatically in 2006 because of an infestation of white sweet clover (*Melilotus alba*) which died out completely and very little green vegetation was left in the field after July. Even though spring 2006 was wet at the Vaira site, NEE decreased substantially in the 2005–2006 growing season because an extraordinary amount of litter produced in 2004–2005 covered the ground surface and suppressed

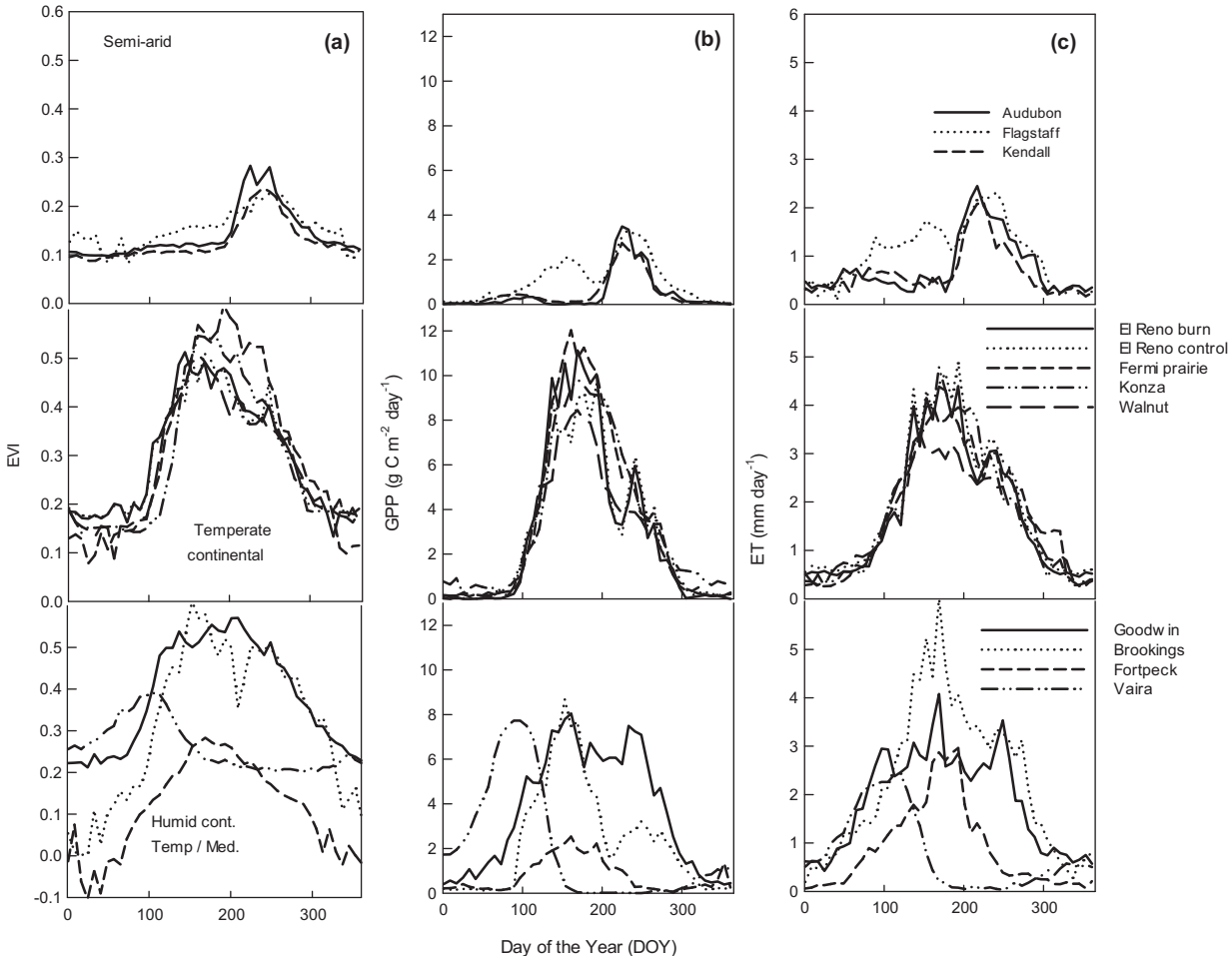

Fig. 2. Mean seasonal dynamics (8-day composite values) of enhanced vegetation index (EVI), gross primary production (GPP), and evapotranspiration (ET) at the 12 grassland sites. Data over the study period were composited into a single year for each site to determine the mean seasonal patterns.

Table 3
Integrated net ecosystem CO_2 exchange (NEE, g C m^{-2} year^{-1}), gross primary production (GPP, g C m^{-2} year^{-1}), and evapotranspiration (ET, mm year^{-1}) on annual (yr) or growing season (GSL) scales at the 12 grassland sites. Ecosystem water use efficiency (g C mm^{-1} ET) on annual ($EWUE_{yr}$) and seasonal ($EWUE_{GSL}$) scales was derived from the ratio between annual and growing season sums of GPP and ET, respectively.

Site	NEE_{yr} (±SD)	GPP_{yr} (±SD)	ET_{yr} (±SD)	$EWUE_{yr}$	NEE_{GSL} (±SD)	GPP_{GSL} (±SD)	ET_{GSL} (±SD)	$EWUE_{GSL}$
Audubon	88 ± 250	178 ± 151	264 ± 10	0.67 ± 0.55	−5 ± 110	147 ± 112	155 ± 35	0.93 ± 0.64
Flagstaff Wildfire	93	391	382	1.02	60	353	302	1.17
Kendall	−20 ± 44	188 ± 66	231 ± 37	0.79 ± 0.19	−39 ± 46	146 ± 67	138 ± 33	1.0 ± 0.3
El Reno burn	−71	1139	651	1.75	−207	1129	563	1.96 ± 0.71
El Reno control	−13	1085	714	1.52	−175	1060	603	1.74 ± 0.29
Fermi Prairie	−333	1298	660	1.97	−389	1267	580	2.23 ± 0.03
Konza	−86 ± 107	1308 ± 303	663 ± 136	1.98 ± 0.3	−186 ± 102	1206 ± 317	593 ± 132	2.03 ± 0.22
Walnut	−118	968	594	1.63	−154	938	510	1.83 ± 0.12
Brookings	−183	859	826	1.04	−181	839	742	1.19 ± 0.52
Fort Peck	9 ± 90	331 ± 178	348 ± 99	0.88 ± 0.37	19 ± 88	238 ± 148	262 ± 124	0.90 ± 0.36
Goodwin	−223 ± 204	1369 ± 261	665 ± 117	2.04 ± 0.37	−233 ± 187	1345 ± 260	636 ± 106	2.14 ± 0.4
Vaira	−55 ± 96	759 ± 204	299 ± 41	2.52 ± 0.52	−127 ± 113	751 ± 202	280 ± 34	2.65 ± 0.43

the grass growth in 2005–2006, and also increased ER (Ma et al., 2007).

3.4. Relationship of EVI with carbon and water vapor fluxes

The EVI was strongly correlated with GPP, with correlation coefficient (r) of more than 0.8 at nine out of 12 sites, and with ET, with r of more than 0.7 at ten out of 12 sites (Table 4). The across-site analysis showed that the correlation of EVI remained high with seasonal variations in GPP (r = 0.85) and ET (r = 0.80). The EVI_{max} was strongly correlated with spatial variations in NEE_{max} (R^2 = 0.67, P = 0.001), GPP_{max}, (R^2 = 0.80, P < 0.001), and ET_{max} (R^2 = 0.68, P < 0.001). To further test the capabilities of EVI to capture the observed trends in the flux data series and seasonal sums of fluxes, we tested the ability of GSL_{EVI} to predict GSL_{GPP} and CUP (Fig. 4a), and seasonal sums of GPP and ET (Fig. 4b). We also examined the relationships of EWUE, GPP, and ET with EVI_{sum} on the seasonal scale (Fig. 4c, d). The GSL_{EVI} showed strong linear correlations with the spatial variability

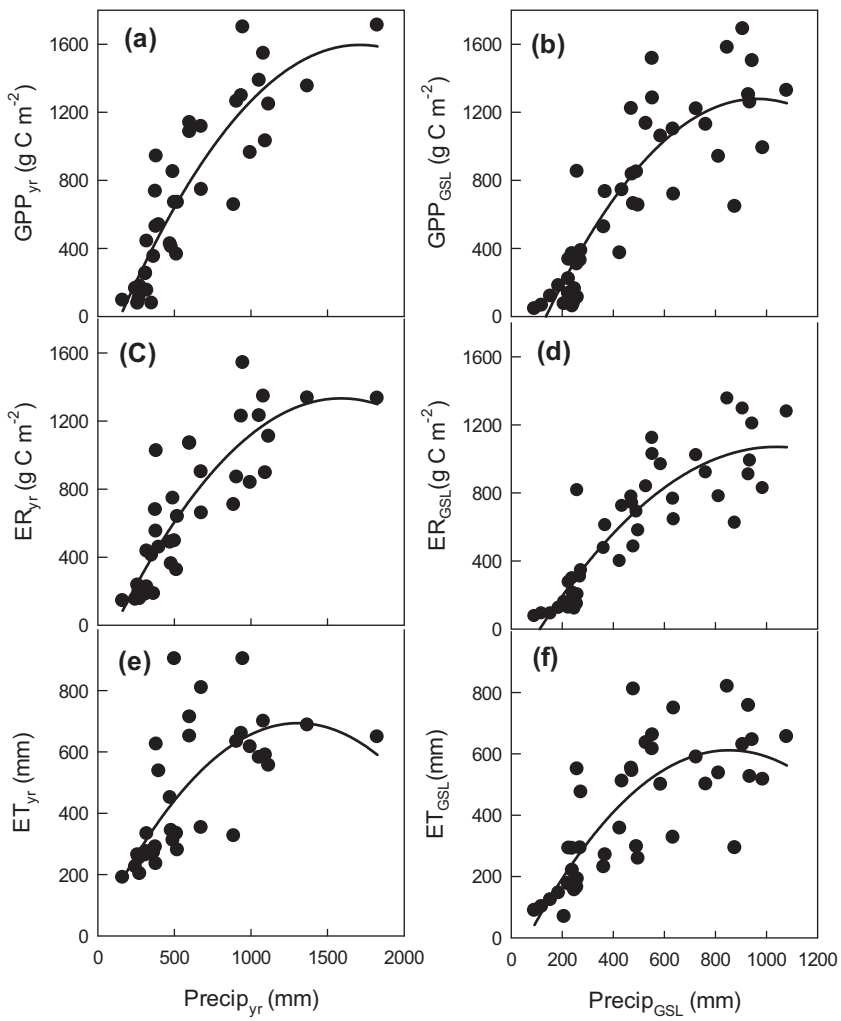

Fig. 3. Relationships of annual (yr) or growing season (GSL) sums of gross primary production (GPP), ecosystem respiration (ER), and evapotranspiration (ET) with annual or seasonal sum of precipitation (Precip): (a) $y = -313 + 2.23x - 0.0007x^2$, $R^2 = 0.79$, (b) $y = -456 + 3.6x - 0.002x^2$, $R^2 = 0.77$, (c) $y = -215 + 1.95x - 0.0006x^2$, $R^2 = 0.74$, (d) $y = -274 + 2.59x - 0.001x^2$, $R^2 = 0.79$, (e) $y = 31.76 + 1.01x - 0.0004x^2$, $R^2 = 0.50$, and (f) $y = -103 + 1.67x - 0.001x^2$, $R^2 = 0.62$. All relationships were statistically significant at the 0.0001 level. Lines represent best fit regressions.

Table 4
Correlation coefficients (r) between 8-day composite values of gross primary production (GPP), evapotranspiration (ET), and enhanced vegetation index (EVI) for the entire study period at the 12 grassland sites.

Site	GPP–EVI	ET–EVI
Audubon	0.90	0.79
Flagstaff Wildfire	0.63	0.47
Kendall	0.85	0.72
El Reno burn	0.94	0.91
El Reno control	0.93	0.92
Fermi Prairie	0.88	0.89
Konza	0.89	0.80
Walnut	0.94	0.92
Brookings	0.73	0.81
Fort Peck	0.69	0.67
Goodwin	0.83	0.78
Vaira	0.87	0.81
Cross-sites	0.85	0.80

in GSL_{GPP} ($R^2 = 0.94$, $P < 0.0001$), CUP ($R^2 = 0.70$, $P < 0.001$), GPP_{GSL} ($R^2 = 0.62$, $P = 0.002$), and ET_{GSL} ($R^2 = 0.61$, $P = 0.003$). High levels of canopy green biomass and coverage, as indicated by higher seasonal EVI_{sum}, were strongly associated with higher $EWUE_{GSL}$ ($R^2 = 0.62$, $P < 0.0001$), GPP_{GSL} ($R^2 = 0.78$, $P < 0.0001$), and ET_{GSL} ($R^2 = 0.73$, $P < 0.0001$) (Fig. 4c, d).

3.5. Relationship between GPP and ET, and variability in EWUE

The across-site analysis of annual or growing season sums of GPP and ET showed strong positive relationships ($R^2 = 0.77$ on an annual scale and $R^2 = 0.82$ on the seasonal scale, Fig. 5), indicating strong coupling between GPP and ET. However, the ratio of sums of GPP to ET yielded variations in $EWUE_{yr}$ (ranged from 0.67 ± 0.55 to 2.52 ± 0.52 g C mm^{-1} ET) and $EWUE_{GSL}$ (ranged from 0.90 ± 0.36 to 2.65 ± 0.43 g C mm^{-1} ET) across study sites (Table 3). We also found interannual variability in EWUE at the same sites. Reduction in GPP during relatively dry years compared to non-dry years at a similar level of ET resulted in a smaller EWUE (i.e., the slope of the relationship between GPP and ET, Fig. 6).

3.6. Response of NEE, GPP, and ET to T_a and VPD

To better understand the effects of climate change on carbon and water vapor fluxes of grassland ecosystems, we compared the response of NEE, GPP, and ET to two major climatic variables (T_a and VPD) among all grassland sites (Fig. 7a, b). Results show that the responses of NEE, GPP, and ET to T_a and VPD varied among grassland sites. In general, NEE, GPP, and ET increased with T_a and VPD up to a certain level and declined thereafter. The optimum ranges of T_a and VPD for NEE, GPP, and ET differed among sites. However, the

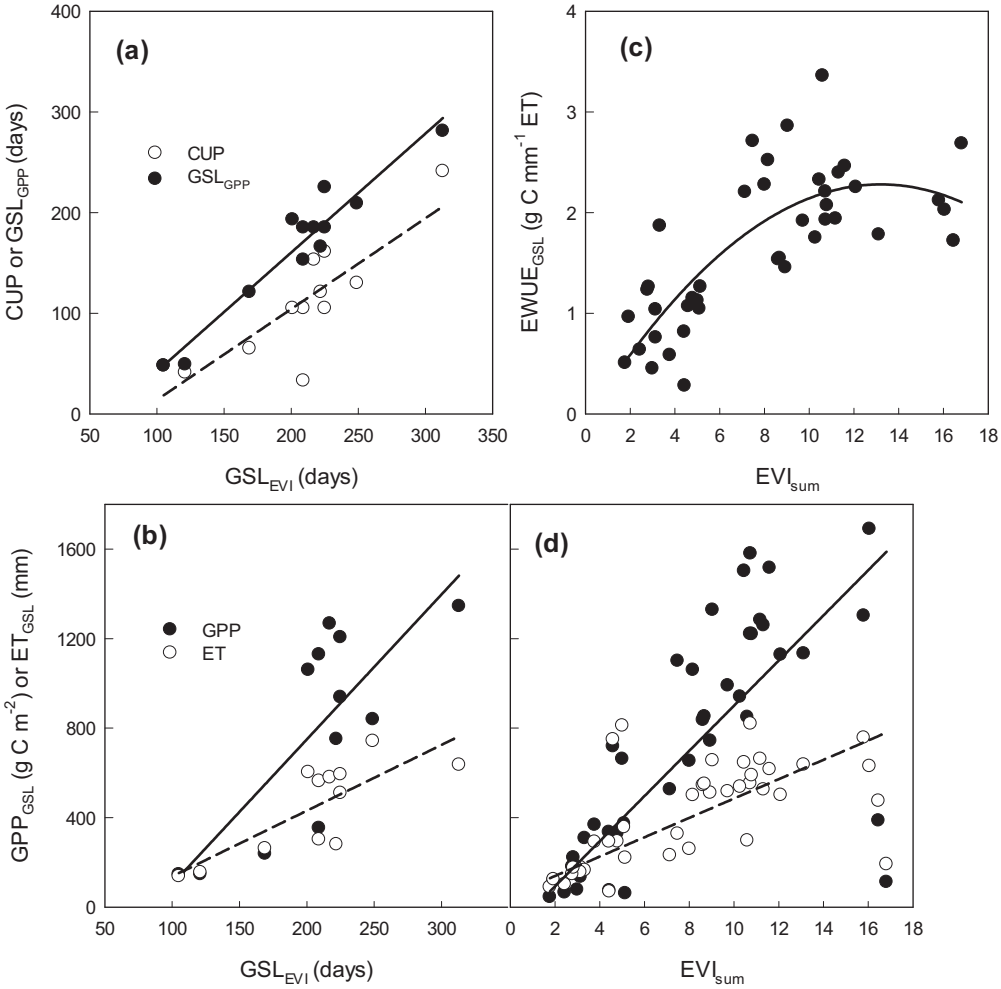

Fig. 4. Relationships between: (a) carbon uptake period (CUP) and growing season lengths based on enhanced vegetation index (GSL_{EVI}) and gross primary production (GSL_{GPP}): $CUP = 0.9x - 76.2$, $R^2 = 0.70$, $P < 0.001$ and $GSL_{GPP} = 1.18x - 76.02$, $R^2 = 0.94$, $P < 0.0001$, (b) GSL_{EVI} and growing season sums of GPP (GPP_{GSL}) and ET (ET_{GSL}): $GPP_{GSL} = 6.48x - 546$, $R^2 = 0.62$, $P = 0.002$ and $ET_{GSL} = 2.94x - 157$, $R^2 = 0.61$, $P = 0.003$, (c) ecosystem water use efficiency ($EWUE_{GSL}$) and sum of enhanced vegetation index (EVI_{sum}) on the seasonal scale: $y = -0.07 + 0.36x - 0.01x^2$, $R^2 = 0.61$, $P < 0.0001$, and (d) GPP_{GSL}, ET_{GSL}, and EVI_{sum}: $GPP_{GSL} = 101x - 109$, $R^2 = 0.78$, $P < 0.0001$ and $ET_{GSL} = 43.3x + 52.7$, $R^2 = 0.73$, $P < 0.0001$. Lines represent best fit regressions.

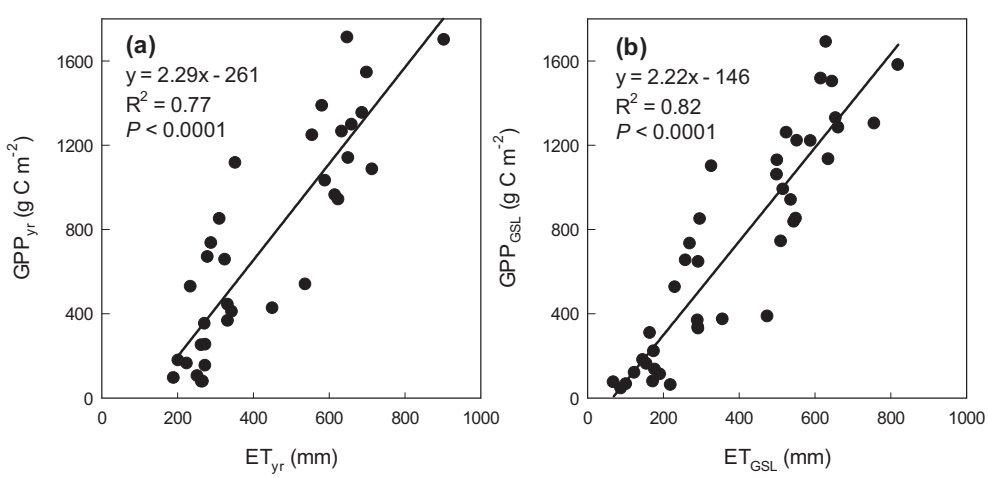

Fig. 5. Relationships between annual (yr) or growing season (GSL) gross primary production (GPP) and evapotranspiration (ET) across the 12 grassland sites. Lines represent best fit linear regressions.

responses of NEE, GPP, and ET to T_a and VPD were very similar among grasslands in the same climatic zone. Maximum values of NEE, GPP, and ET occurred at about 22–23 °C at two semi-arid sites (Flagstaff Wildfire and Kendall), while they occurred at ~27 °C at another semi-arid site (Audubon). Maximum values of NEE and GPP occurred at ~25 °C and ET occurred at ~30 °C at Fermi Prairie, while NEE and GPP peaked at ~30 °C and ET peaked at ~35 °C at all other four temperature continental sites and Goodwin (temperate). The

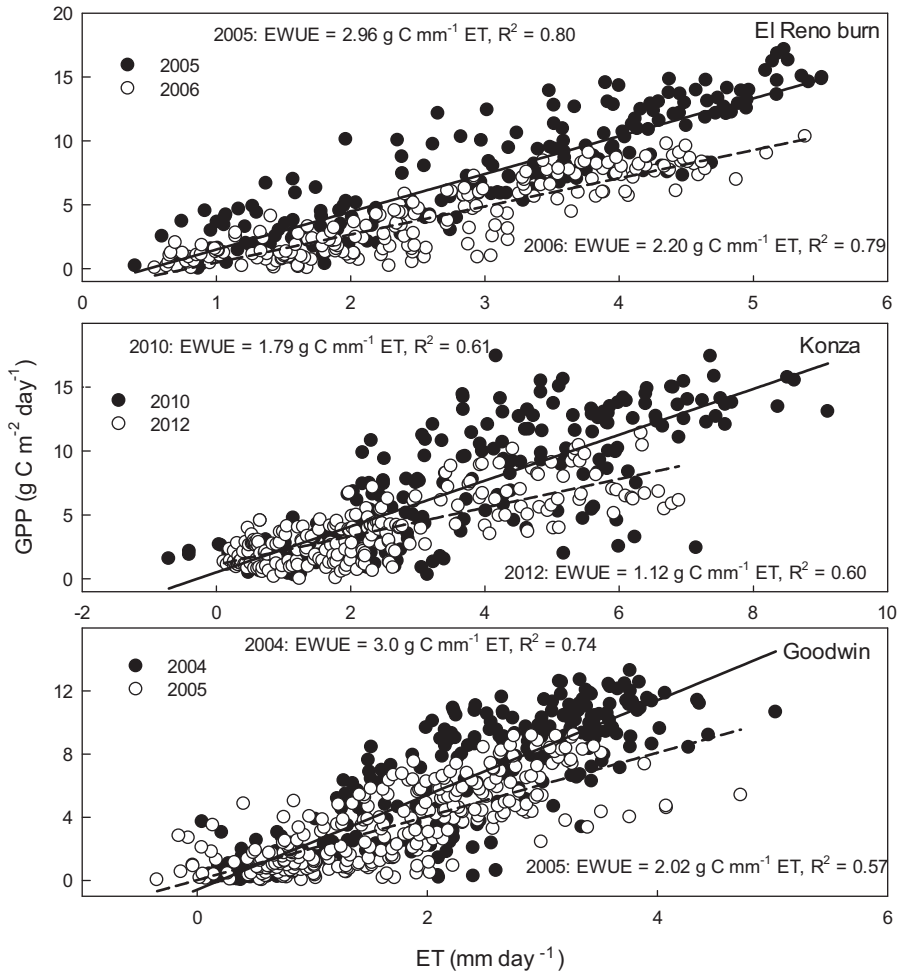

Fig. 6. Ecosystem water use efficiency (EWUE), i.e., the slope of gross primary production (GPP) vs. evapotranspiration (ET) on daily basis in dry (open symbols and dotted lines) and non-dry years (closed symbols and solid lines) for the three selected grassland sites.

NEE and GPP peaked at ~25 °C and ET at ~30 °C at Brookings and Fort Peck. Maximum values of NEE, GPP, and ET occurred at ~20 °C at Vaira (Mediterranean).

Maximum values of NEE, GPP, and ET occurred at about VPD of 15–17 hPa and depressed when VPD > 20 hPa at all three semi-arid sites. The values reached maximum at ~27 hPa at three temperate continental sites (El Reno burn, El Reno control, and Konza), while they were maximum at ~20 hPa at Walnut and ~15 hPa at Fermi Prairie. Both NEE and GPP reached maximum at ~10 hPa at Brookings, Fort Peck, and Vaira, while they reached maximum at ~18 hPa at Goodwin. The ET reached maximum at ~25 hPa at Brookings, ~20 hPa at two temperate sites (Fort Peck and Goodwin), and at ~15 hPa at Vaira. Our results show that carbon fluxes and ET responded to T_a and VPD differently. Lower optimum temperature ranges for NEE and GPP than ET, and more decline in NEE and GPP than ET at high T_a and VPD across sites (Fig. 7a, b) indicated that physiological controls in response to increased T_a and VPD more greatly affected NEE and GPP than ET.

As the individual response of GPP and ET to climatic variables may be confounded by the effect of VPD on canopy conductance, we also compared the relationship between GPP and ET vs. GPP × VPD and ET at the three selected sites in different climatic zones during relatively dry years (Fig. 8). As expected, GPP and ET showed a linear relationship, but interestingly the relationship between GPP × VPD and ET was exponential across all sites. The linear relationship (R^2 = 0.82) between GPP and ET was only slightly weaker than the exponential relationship (R^2 = 0.84) between GPP × VPD and ET at the El Reno control site, but the exponential relationship between GPP × VPD and ET was substantially stronger than the linear relationship between GPP and ET at Fort Peck (R^2 = 0.70 vs. 0.55) and Vaira (R^2 = 0.86 vs. 0.78).

4. Discussion

4.1. Variability in EVI and carbon and water vapor fluxes

The considerable effects of precipitation and SWC on vegetation production, as indicated by EVI values, were consistent with previous reports that higher precipitation promotes higher biomass in grasslands across spatial scales (Bai et al., 2004; Sala et al., 1988). This enhanced plant growth and productivity was strongly correlated with greater rates of carbon and water vapor fluxes, showing the ability of EVI to track spatial variability in carbon and water vapor fluxes of geographically distributed grasslands. Our analysis also demonstrates that EVI can be used to delineate growing season length and CUP, and to approximate carbon and water vapor fluxes, and EWUE of grasslands (Fig. 4). These results indicate much potential of using this EVI approach for understanding and extrapolating fluxes over large grassland areas. A previous study also showed the potential to link the MODIS EVI and tower-derived GPP to better understand the functioning of savanna ecosystems across the north Australian tropical transect (Ma et al., 2013). Similarly, Churkina et al. (2005) showed that EVI calculated from VEGETATION SPOT-4

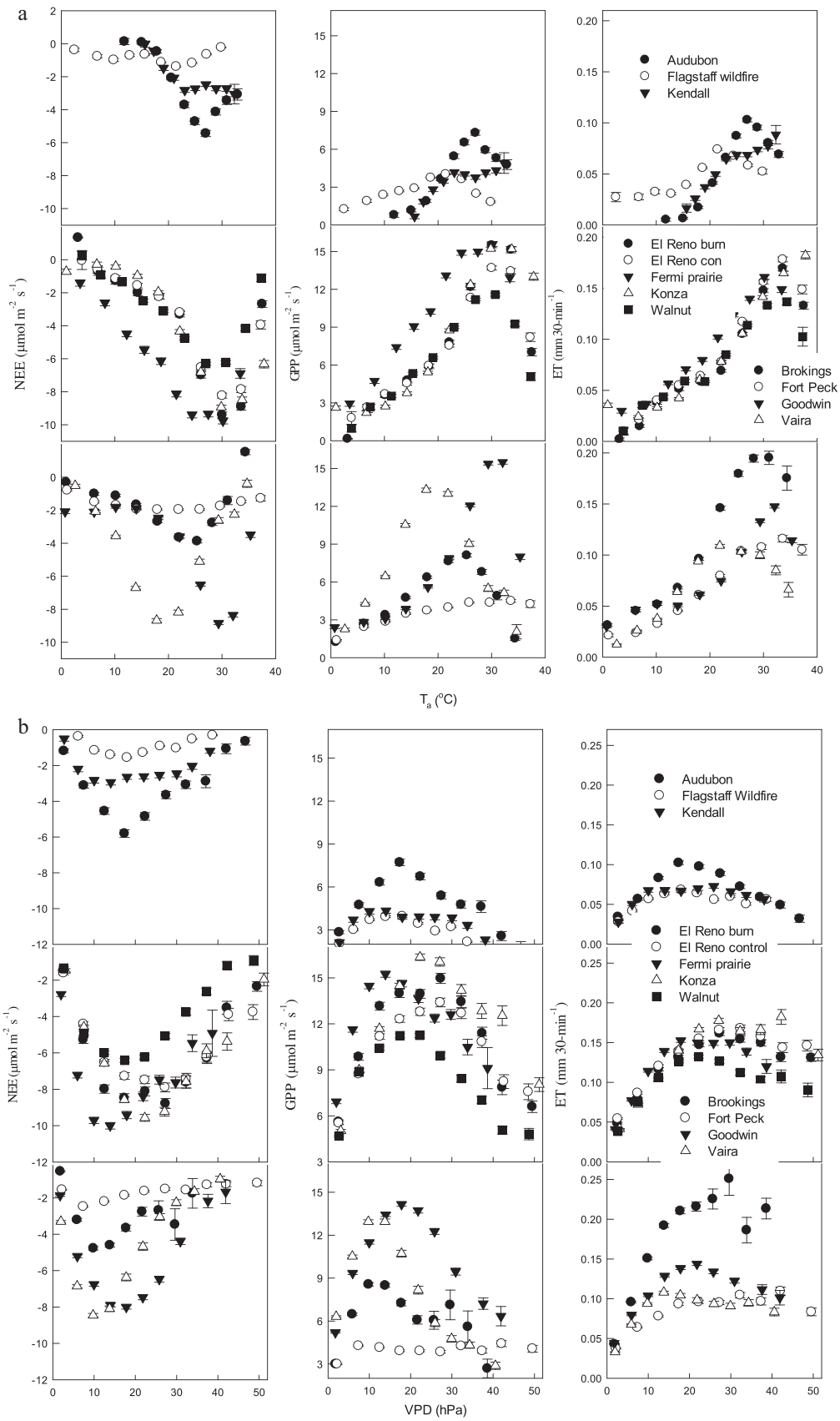

Fig. 7. Response of net ecosystem exchange (NEE), gross primary production (GPP), and evapotranspiration (ET) to (a) air temperature (T_a) and (b) vapor pressure deficit (VPD) at the 12 grassland sites. Half-hourly NEE, GPP, and ET data during day time (global radiation >5 W m^{-2}) for the entire study period were aggregated in classes of increasing T_a and VPD.

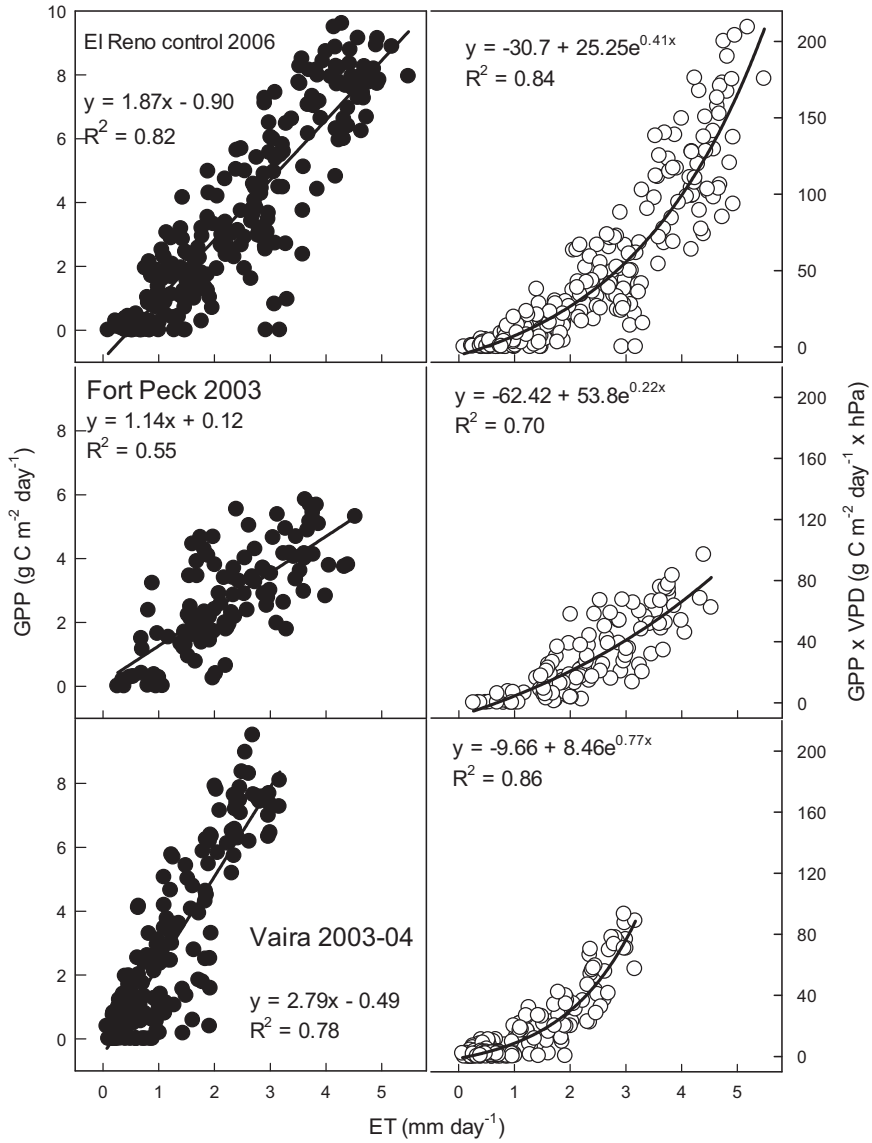

Fig. 8. Relationship between gross primary production (GPP) and evapotranspiration (ET), and between GPP × VPD (vapor pressure deficit) and ET on a daily basis for the selected sites during dry years.

was strongly correlated to the CUP and could be utilized to estimate NEE_{yr} of a broad range of ecosystems.

Our results illustrate that the carbon uptake-emission status of the grasslands was conditional upon soil water availability and precipitation. Higher annual average θ_R was strongly correlated with higher values of fluxes. Similarly, carbon fluxes and ET increased linearly with increasing precipitation at lower ranges of precipitation (<1000 mm of annual rainfall and <600 mm of seasonal rainfall) (Fig. 3). This result supports an earlier finding (Gilmanov et al., 2005) that mixed prairie ecosystems in North America emitted more carbon than they assimilated during years with lower than normal rainfall. A study that manipulated rainfall variability and quantity in a C_4 dominated native grassland in Northeast Kansas showed that carbon cycling processes such as soil carbon efflux and carbon uptake by the vegetation were suppressed when rainfall variability increased (Knapp et al., 2002). These results indicate that projected increases in rainfall variability due to anthropogenic climate change and atmospheric warming could greatly influence carbon cycling processes of grasslands. Further, our study shows that carbon dynamics of grasslands were subject to disturbance events (*i.e.*, fire, invasion) and the biological legacy effects of one year on another year. Such alterations in carbon dynamics have been reported for several grassland and forest ecosystems worldwide (Amiro et al., 2006; Barr et al., 2007; Ciais et al., 2005; Flanagan et al., 2002; Gilmanov et al., 2007). These results suggest that this interannual variability in carbon and water vapor fluxes of ecosystems should be considered when estimating regional carbon and water budgets.

4.2. Coupling between GPP and ET, and variability in EWUE

As expected, GPP and ET were strongly correlated (Fig. 5) due to the physiological control of gas exchange (Valentini et al., 1991). However, responses to seasonal variations in climatic variables differed between GPP and ET. These differential responses presumably led to partial decoupling between GPP and ET under changing environmental conditions. As a result, the relationship between GPP and ET was weaker as compared to GPP × VPD and ET among selected sites in different climatic zones in relatively dry years (Fig. 8). These results demonstrate that the intrinsic link between carbon assimilation and water loss through stomatal conductance exists in grasslands at the ecosystem level since the ratio of ET to VPD

is a proxy for canopy conductance (Beer et al., 2009). As in Beer et al. (2009), we also observed a nonlinear relationship between GPP × VPD and ET for grasslands, suggesting greater decoupling of herbaceous canopies from the atmosphere than forests (Jarvis and McNaughton, 1986).

The climatic gradient affected grassland phenology and canopy coverage across study sites, which strongly influenced carbon and water vapor fluxes of grasslands. The GPP_{GSL} and ET_{GSL} were strongly correlated with EVI_{sum}, and additional units of EVI were associated with a greater increase in GPP_{GSL} (101 g C m^{-2}) than ET_{GSL} (43.3 mm) as shown in Fig. 4d. This is likely because increasing canopy coverage increased light use efficiency for photosynthesis and attenuated radiation transmitted to the soil surface and reduced soil evaporation. Although both GPP and ET decreased during dry conditions, drought-induced reduction in vegetation cover along with leaf-level physiological controls of high T_a and VPD on GPP than on ET caused more reduction in GPP than in ET. As a result, EWUE was higher at the sites with larger EVI and less climatically imposed water limitation, and it was lower in dry years (Fig. 6) and at sites with smaller EVI (Fig. 4c). Our result supports the finding of a previous study (Hu et al., 2008) which showed a reduction in EWUE during drought and high EWUE in the years or sites with high productivity of Chinese temperate grasslands. These results show a pronounced effect of drought on carbon and water vapor fluxes and EWUE of grasslands.

Reduction in EWUE of grasslands during drought in this study indicated the opposite response than what has generally been reported for forests. Previous studies in forest ecosystems have shown that EWUE of forests increases in dry years because of a greater reduction in ET than GPP. During drought, EWUE increased in European forests but not in grasslands (Wolf et al., 2013). Krishnan et al. (2006) reported a larger relative reduction in ET than in GPP of boreal forests in Saskatchewan, Canada, leading to higher EWUE in dry years. Likewise, fairly constant values of EWUE were observed in most of the coniferous boreal and temperate forests of Canada (Brümmer et al., 2012). Water use efficiency in a beech forest was mainly controlled by evaporative demand of the atmosphere and leaf stomatal behavior, and not by the canopy coverage (Herbst et al., 2002). In contrast, higher EWUE of grasslands was associated with higher EVI in our study (Fig. 4c). This contrasting result can be attributed to differences in soil evaporation as soil evaporation is negligible under well-developed forest but considerable in grasslands. Previous studies reported that grasslands did not reduce ET as long as soil moisture was available but forests employed water saving strategies by reducing ET, causing the contrasting responses of European forests and grasslands to drought and heatwaves (Teuling et al., 2010; Wolf et al., 2013). These results suggest that the current ecosystem modeling approaches which predict increasing EWUE in response to drought (Baldocchi, 1997; Schulze, 1986; Williams et al., 1998) under the assumption of more stomatal regulation of water losses with slight reductions in photosynthesis (Flexas and Medrano, 2002) might not be applicable for all biomes, at least for grasslands. This indicates the need to consider reduction in EWUE during drought when modeling carbon fluxes of grasslands, especially in drought-prone environments.

5. Conclusions

This study revealed large spatial variability in carbon and water vapor fluxes, and vegetation properties such as EVI among geographically distributed grasslands in the U.S. These variations were primarily related to differences in precipitation and soil water availability. Integration of EVI with ground-based eddy flux and climate data showed potential to improve understanding of the temporal and spatial variability in carbon and water vapor fluxes, and to approximate GSL, CUP, EWUE, and carbon and water vapor fluxes of grasslands. However, this result needs verification by long-term observations across geographical sites and by more complete sampling of grasslands of the world to examine whether these relationships hold. For example, this study lacks data from grasslands in tropical and sub-tropical regions. Our results show that the optimum T_a and VPD ranges were lower for NEE and GPP than for ET, and NEE and GPP were reduced more than ET at high T_a and VPD, suggesting the higher sensitivity of NEE and GPP than ET to aridity. As a result, EWUE of grasslands decreased during dry years, a response the opposite of what has generally been reported in forest ecosystems. This result is inconsistent with the assumption of current models of canopy functions which predict increasing EWUE during drought due to a reduction in stomatal conductance. An evaluation of the intrinsic link between GPP and ET through stomatal conductance across a wide range of environmental conditions is essential to better understand adaptation mechanisms of grasslands to climate. Our study's comparison of the responses of carbon and water vapor fluxes of geographically distributed grasslands to major climatic variables provides insight about the effects of climate change on carbon and water budgets of grasslands.

Acknowledgements

This study was supported in part by a research grant (Project No. 2012-02355) through the USDA National Institute for Food and Agriculture (NIFA)'s Agriculture and Food Research Initiative (AFRI), Regional Approaches for Adaptation to and Mitigation of Climate Variability and Change, and a research grant (IIA-1301789) from the National Science Foundation EPSCoR. This research was supported by grants to T. Kolb and Northern Arizona University from the North American Carbon Program/USDA CREES NRI (2004-35111-15057 and 2008-35101-19076) and Science Foundation Arizona (CAA 0-203-08). The Konza Prairie site was supported by grants to N. Brunsell from the NSF EPSCoR (NSF EPS-0553722 and EPS-0919443) and KAN0061396/KAN0066263 and the NSF Long Term Ecological Research Program at Konza Prairie Biological Station (DEB-0823341 and sub-contract: SS1093). It was also partly supported by NOAA Climate Program Office's Sectoral Applications Research Program (SARP) grant NA130AR4310122. The Fermi site was supported by the U.S. Department of Energy, Office of Science, Office of Biological and Environmental Research, Terrestrial Ecosystem Science Program under contract DE-AC02-06CH11357. Funding for the Kendall and Santa Rite flux sites was from the USDA and U.S. Department of Energy's Office of Science. Data were obtained from AmeriFlux database (http://ameriflux.ornl.gov/). The authors thank an anonymous reviewer for the comments on previous version of this manuscript.

References

Amiro, B., et al., 2006. Carbon, energy and water fluxes at mature and disturbed forest sites Saskatchewan, Canada. Agric. For. Meteorol. 136 (3), 237–251.
Bai, Y., Han, X., Wu, J., Chen, Z., Li, L., 2004. Ecosystem stability and compensatory effects in the Inner Mongolia grassland. Nature 431 (7005), 181–184.
Baldocchi, D., 1997. Measuring and modelling carbon dioxide and water vapour exchange over a temperate broad-leaved forest during the 1995 summer drought. Plant Cell Environ. 20 (9), 1108–1122.
Baldocchi, D.D., Xu, L., Kiang, N., 2004. How plant functional-type, weather, seasonal drought, and soil physical properties alter water and energy fluxes of an oak–grass savanna and an annual grassland. Agric. For. Meteorol. 123 (1), 13–39.
Barr, A.G., et al., 2007. Climatic controls on the carbon and water balances of a boreal aspen forest, 1994–2003. Glob. Change Biol. 13 (3), 561–576.
Beer, C., et al., 2009. Temporal and among-site variability of inherent water use efficiency at the ecosystem level. Glob. Biogeochem. Cycles 23 (2).
Biondini, M.E., Lauenroth, W.K., Sala, O.E., 1991. Correcting estimates of net primary production: are we overestimating plant production in rangelands. J. Range Manage. 44 (3), 194–198.

Brümmer, C., et al., 2012. How climate and vegetation type influence evapotranspiration and water use efficiency in Canadian forest, peatland and grassland ecosystems. Agric. For. Meteorol. 153, 14–30.
Brunsell, N.A., Ham, J.M., Owensby, C.E., 2008. Assessing the multi-resolution information content of remotely sensed variables and elevation for evapotranspiration in a tall-grass prairie environment. Remote Sens. Environ. 112 (6), 2977–2987.
Burkett, V.R., et al., 2005. Nonlinear dynamics in ecosystem response to climatic change: case studies and policy implications. Ecol. Complex. 2 (4), 357–394.
Churkina, G., Schimel, D., Braswell, B.H., Xiao, X., 2005. Spatial analysis of growing season length control over net ecosystem exchange. Glob. Change Biol. 11 (10), 1777–1787.
Ciais, P., et al., 2005. Europe-wide reduction in primary productivity caused by the heat and drought in 2003. Nature 437 (7058), 529–533.
DeForest, J.L., et al., 2006. Phenophases alter the soil respiration–temperature relationship in an oak-dominated forest. Int. J. Biometeorol. 51 (2), 135–144.
Dore, S., et al., 2008. Long-term impact of a stand-replacing fire on ecosystem CO_2 exchange of a ponderosa pine forest. Glob. Change Biol. 14 (8), 1801–1820.
Falge, E., et al., 2002. Phase and amplitude of ecosystem carbon release and uptake potentials as derived from FLUXNET measurements. Agric. For. Meteorol. 113 (1), 75–95.
Fischer, M.L., et al., 2012. Carbon, water, and heat flux responses to experimental burning and drought in a tallgrass prairie. Agric. For. Meteorol. 166, 169–174.
Flanagan, L.B., Wever, L.A., Carlson, P.J., 2002. Seasonal and interannual variation in carbon dioxide exchange and carbon balance in a northern temperate grassland. Glob. Change Biol. 8 (7), 599–615.
Flexas, J., Medrano, H., 2002. Drought-inhibition of photosynthesis in C3 plants: stomatal and non-stomatal limitations revisited. Ann. Bot. 89 (2), 183–189.
Gill, R.A., et al., 2002. Nonlinear grassland responses to past and future atmospheric CO_2. Nature 417 (6886), 279–282.
Gilmanov, T., et al., 2007. Partitioning European grassland net ecosystem CO_2 exchange into gross primary productivity and ecosystem respiration using light response function analysis. Agric. Ecosyst. Environ. 121 (1), 93–120.
Gilmanov, T.G., et al., 2010. Productivity, respiration, and light-response parameters of world grassland and agroecosystems derived from flux-tower measurements. Rangel. Ecol. Manage. 63 (1), 16–39.
Gilmanov, T.G., et al., 2005. Integration of CO_2 flux and remotely-sensed data for primary production and ecosystem respiration analyses in the Northern Great Plains: potential for quantitative spatial extrapolation. Glob. Ecol. Biogeogr. 14 (3), 271–292.
Gilmanov, T.G., et al., 2003. Gross primary production and light response parameters of four Southern Plains ecosystems estimated using long-term CO_2-flux tower measurements. Glob. Biogeochem. Cycles 17 (2).
Herbst, M., Kutsch, W.L., Hummelshøj, P., Jensen, N.O., Kappen, L., 2002. Canopy physiology: interpreting the variations in eddy fluxes of water vapour and carbon dioxide observed over a beech forest. Basic Appl. Ecol. 3 (2), 157–169.
Hu, Z., et al., 2008. Effects of vegetation control on ecosystem water use efficiency within and among four grassland ecosystems in China. Glob. Change Biol. 14 (7), 1609–1619.
Huete, A., et al., 2002. Overview of the radiometric and biophysical performance of the MODIS vegetation indices. Remote Sens. Environ. 83 (1), 195–213.
Hutyra, L.R., et al., 2007. Seasonal controls on the exchange of carbon and water in an Amazonian rain forest. J. Geophys. Res.: Biogeosci. (2005–2012) 112 (G3).
Huxman, T.E., et al., 2004. Convergence across biomes to a common rain-use efficiency. Nature 429 (6992), 651–654.
Jarvis, P.G., McNaughton, K., 1986. Stomatal control of transpiration: scaling up from leaf to region. Adv. Ecol. Res. 15, 1–49.
Kato, T., Tang, Y., 2008. Spatial variability and major controlling factors of CO_2 sink strength in Asian terrestrial ecosystems: evidence from eddy covariance data. Glob. Change Biol. 14 (10), 2333–2348.
Knapp, A.K., et al., 2002. Rainfall variability, carbon cycling, and plant species diversity in a mesic grassland. Science 298 (5601), 2202–2205.
Krishnan, P., et al., 2006. Impact of changing soil moisture distribution on net ecosystem productivity of a boreal aspen forest during and following drought. Agric. For. Meteorol. 139 (3), 208–223.
Krishnan, P., Meyers, T.P., Scott, R.L., Kennedy, L., Heuer, M., 2012. Energy exchange and evapotranspiration over two temperate semi-arid grasslands in North America. Agric. For. Meteorol. 153, 31–44.
Law, B., et al., 2002. Environmental controls over carbon dioxide and water vapor exchange of terrestrial vegetation. Agric. For. Meteorol. 113 (1), 97–120.
Ma, S., Baldocchi, D.D., Xu, L., Hehn, T., 2007. Inter-annual variability in carbon dioxide exchange of an oak/grass savanna and open grassland in California. Agric. For. Meteorol. 147 (3), 157–171.
Ma, X., et al., 2013. Spatial patterns and temporal dynamics in savanna vegetation phenology across the North Australian Tropical Transect. Remote Sens. Environ. 139, 97–115.
Matamala, R., Jastrow, J.D., Miller, R.M., Garten, C., 2008. Temporal changes in C and N stocks of restored prairie: implications for C sequestration strategies. Ecol. Appl. 18 (6), 1470–1488.
Myneni, R.B., Keeling, C., Tucker, C., Asrar, G., Nemani, R., 1997. Increased plant growth in the northern high latitudes from 1981 to 1991. Nature 386 (6626), 698–702.
Rahman, A.F., Gamon, J.A., Fuentes, D.A., Roberts, D.A., Prentiss, D., 2001. Modeling spatially distributed ecosystem flux of boreal forest using hyperspectral indices from AVIRIS imagery. J. Geophys. Res.: Atmos. (1984–2012) 106 (D24), 33579–33591.
Reichstein, M., et al., 2005. On the separation of net ecosystem exchange into assimilation and ecosystem respiration: review and improved algorithm. Glob. Change Biol. 11 (9), 1424–1439.
Richardson, A.D., et al., 2010. Influence of spring and autumn phenological transitions on forest ecosystem productivity. Philos. Trans. R. Soc. B: Biol. Sci. 365 (1555), 3227–3246.
Running, S.W., Hunt, E.R., 1993. Generalization of a forest ecosystem process model for other biomes, BIOME-BGC, and an application for global-scale models. In: Scaling Physiological Processes: Leaf to Globe., pp. 141–158.
Sala, O.E., Parton, W.J., Joyce, L., Lauenroth, W., 1988. Primary production of the central grassland region of the United States. Ecology 69 (1), 40–45.
Schulze, E., 1986. Carbon dioxide and water vapor exchange in response to drought in the atmosphere and in the soil. Annu. Rev. Plant Physiol. 37 (1), 247–274.
Scott, R.L., Hamerlynck, E.P., Jenerette, G.D., Moran, M.S., Barron-Gafford, G.A., 2010. Carbon dioxide exchange in a semidesert grassland through drought-induced vegetation change. J. Geophys. Res.: Biogeosci. (2005–2012) 115 (G3).
Song, J., Liao, K., Coulter, R.L., Lesht, B.M., 2005. Climatology of the low-level jet at the Southern Great Plains atmospheric boundary layer experiments site. J. Clim. Appl. Meteorol. 44 (10).
Soussana, J., et al., 2007. Full accounting of the greenhouse gas (CO_2, N_2O, CH_4) budget of nine European grassland sites. Agric. Ecosyst. Environ. 121 (1), 121–134.
Suyker, A.E., Verma, S.B., Burba, G.G., 2003. Interannual variability in net CO_2 exchange of a native tallgrass prairie. Glob. Change Biol. 9 (2), 255–265.
Teuling, A.J., et al., 2010. Contrasting response of European forest and grassland energy exchange to heatwaves. Nat. Geosci. 3 (10), 722–727.
Turner, D.P., et al., 2003. Scaling gross primary production (GPP) over boreal and deciduous forest landscapes in support of MODIS GPP product validation. Remote Sens. Environ. 88 (3), 256–270.
Valentini, R., Scarascia Mugnozza, G., ANGELLS, P., Bimbi, R., 1991. An experimental test of the eddy correlation technique over a Mediterranean macchia canopy. Plant Cell Environ. 14 (9), 987–994.
Wagle, P., Xiao, X., Suyker, A.E., 2015. Estimation and analysis of gross primary production of soybean under various management practices and drought conditions. ISPRS J. Photogramm. Remote Sens. 99, 70–83.
Wagle, P., et al., 2014. Sensitivity of vegetation indices and gross primary production of tallgrass prairie to severe drought. Remote Sens. Environ. 152, 1–14.
Williams, M., et al., 1998. Seasonal variation in net carbon exchange and evapotranspiration in a Brazilian rain forest: a modelling analysis. Plant Cell Environ. 21 (10), 953–968.
Wolf, S., et al., 2013. Contrasting response of grassland versus forest carbon and water fluxes to spring drought in Switzerland. Environ. Res. Lett. 8 (3), 035007.
Xiao, J., et al., 2014. Data-driven diagnostics of terrestrial carbon dynamics over North America. Agric. For. Meteorol. 197, 142–157.
Xiao, J., et al., 2008. Estimation of net ecosystem carbon exchange for the conterminous United States by combining MODIS and AmeriFlux data. Agric. For. Meteorol. 148 (11), 1827–1847.
Yu, G.R., et al., 2013. Spatial patterns and climate drivers of carbon fluxes in terrestrial ecosystems of China. Glob. Change Biol. 19 (3), 798–810.
Yuan, W., et al., 2009. Latitudinal patterns of magnitude and interannual variability in net ecosystem exchange regulated by biological and environmental variables. Glob. Change Biol. 15 (12), 2905–2920.
Zhang, X., et al., 2003. Monitoring vegetation phenology using MODIS. Remote Sens. Environ. 84 (3), 471–475.